Mutant *LRRK2*^{R1441G} BAC Transgenic Mice Recapitulate Cardinal Features of Parkinson's Disease

Yanping Li1*, Wencheng Liu1*, Tinmarla F. Oo, Lei Wang, Yi Tang, Vernice Jackson-Lewis, Chun Zhou, Kindiya Geghman, Mikhail Bogdanov, Serge Przedborski, M. Flint Beal, Robert E. Burke, and Chenjian Li

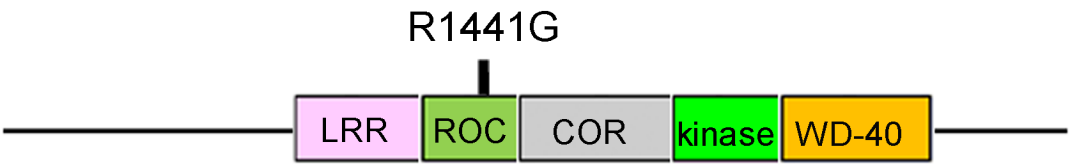

Supplementary Fig. 1 R1441G mutation in LRRK2. A schematic depiction of the human LRRK2 protein LRR, ROC, COR, kinase and WD-40 domains, and the location of the R1441G mutation.

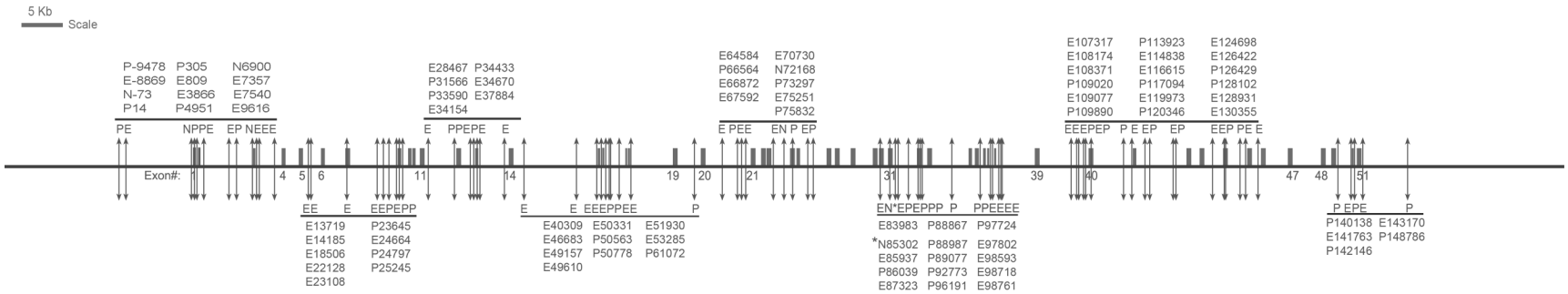

Supplementary Fig. 2 *LRRK2* gene structure and restriction sites. A schematic depiction of the exon-intron structures of the *LRRK2* gene, and the positions of the restriction enzyme sites. The horizontal line represents BAC DNA insert. Boxes on the line represent exons. The translation initiation codon ATG is numbered as 1. Arrowhead lines indicate restriction sites (E: EcoRI; P: PvuII; N: NaeI). The numbers following E, P and N pinpoint the precise positions of restriction sites. The asterisk points to the new NaeI site which was created by introducing *R1441G* mutation.

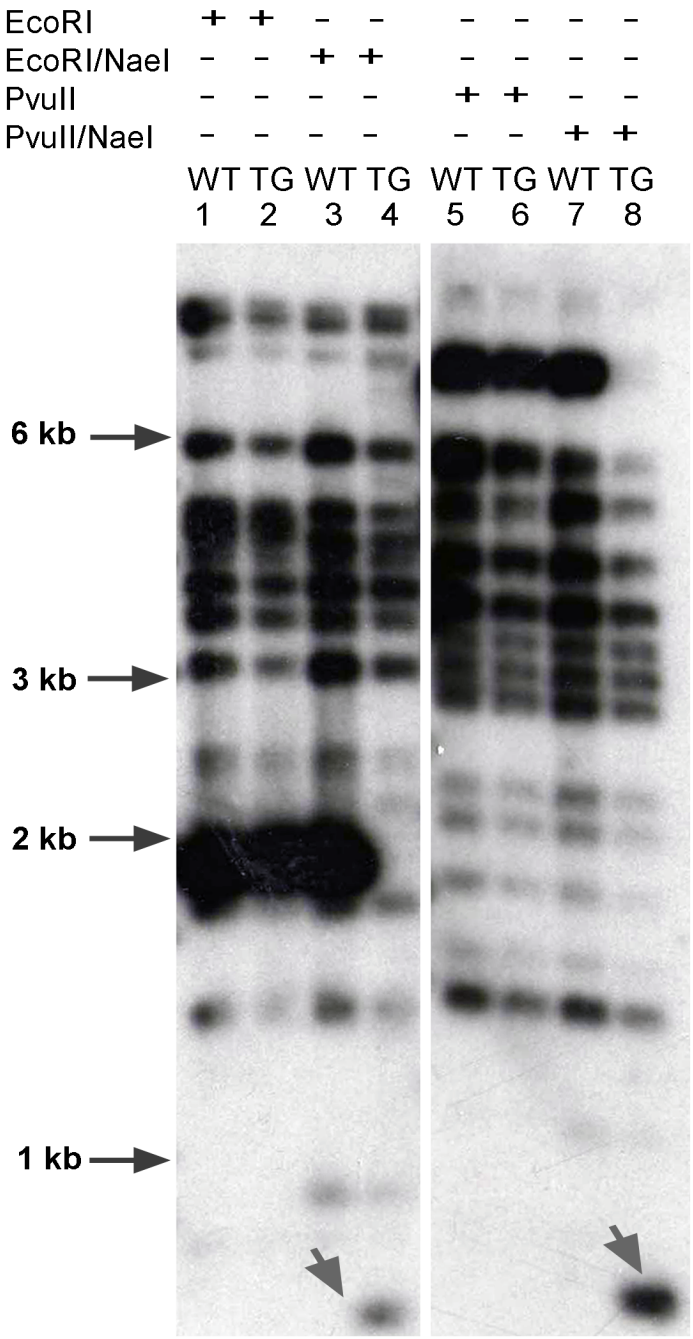

Supplementary Fig. 3 DNA fingerprinting analyses of modified *LRRK2*^{R1441G} BAC by restriction fragment length polymorphism. A blot containing wild type (WT) and *LRRK2*^{R1441G} BAC digested with different combination of restriction enzymes (on the top) was hybridized with human ^{32}P-labeled *LRRK2* cDNA and the resulting autoradiograph is shown. A Nae I site (GCCGGC) was introduced into the *LRRK2*^{R1441G} modified BAC (Supplementary Fig. 4). Nae I digestion of the modified *LRRK2*^{R1441G} BAC produced an additional fragment of an expected size compared to that of the wild type BAC (arrows; compare lane 3 to 4, and lane 7 to 8). No other unwanted re-arrangements or deletions were observed (compare lane 1 to 2, and 5 to **6).**

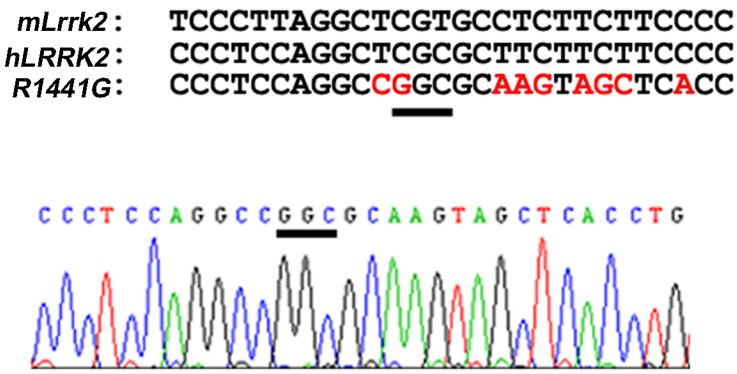

Supplementary Fig. 4. Sequence confirmation of tail DNA from *LRRK2*^{R1441G} BAC transgenic mice. The upper panel is a sequence alignment of endogenous mouse (top), wild type human (middle), and the modified *LRRK2*^{R1441G} (bottom). The modified nucleotides are labeled in red. The sequence corresponding to the *R1441G* mutation is underlined. Silent nucleotide substitutions were also introduced to create an Nae I (GCCGGC) restriction site for convenient identification of the modified *LRRK2*. The lower panel is a trace file of direct tail DNA sequencing of the *LRRK2*^{R1441G} BAC transgenic mouse, showing a perfect match to the designed nucleotide substitutions.

Nature Neuroscience: doi:10.1038/nn.2349

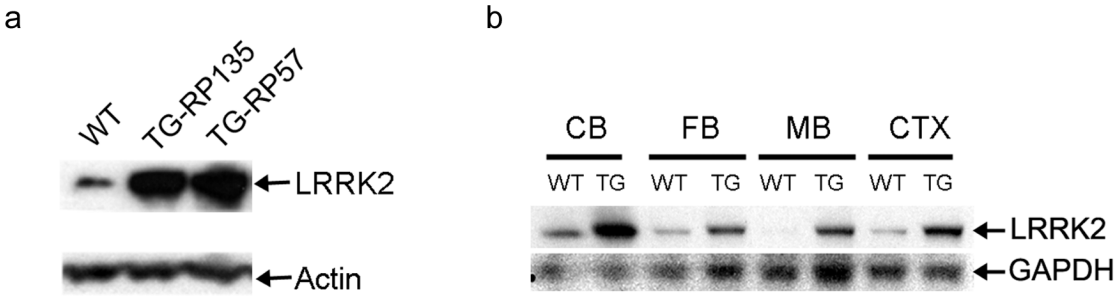

Supplementary Fig. 5 Western analyses of human LRRK2 expression in different lines of *LRRK2*^{R1441G} BAC transgenic mice. (a) Western blot containing brain lysates from wild type non-transgenic mouse (WT) and two lines of *LRRK2*^{R1441G} BAC transgenic mice (TG-RP135 and TG-RP57) was probed with anti-LRRK2 Ab (top panel). The expression levels of LRRK2^{R1441G} are ~5 times higher than that of the endogenous mouse LRRK2. (b) Expression of the LRRK2^{R1441G} in different brain regions of TG and WT mice. Transgene LRRK2^{R1441G} is overexpressed in cortex, forebrain, midbrain, and cerebellum. Actin or GAPDH antibodies were used for normalizing total proteins (bottom panel in a or b). CB: cerebellum; FB: forebrain; MB: midbrain; CTX: cortex

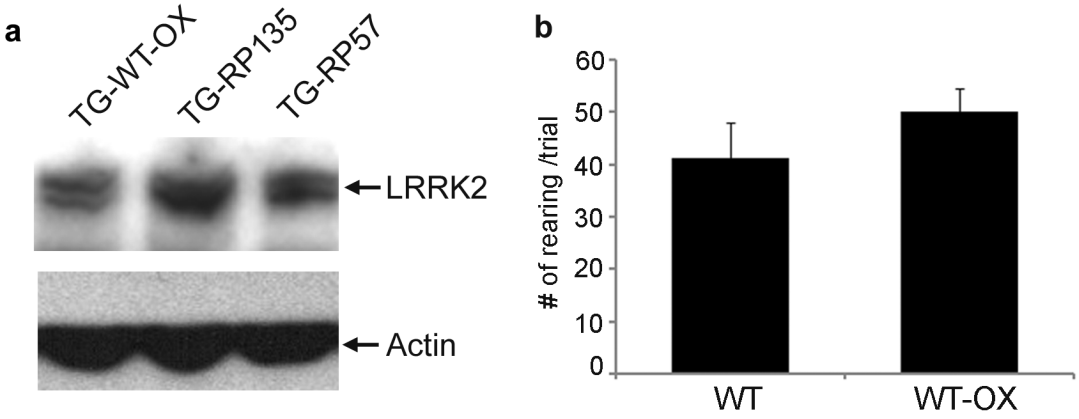

Supplementary Figure 6. Wild type *LRRK2* (WT-OX) BAC mice do not develop age-dependent motor deficits. (a) Western blot containing brain lysates from WT-OX and two lines of *LRRK2*^{R1441G} BAC transgenic mice (TG-RP135 and TG-RP57) was probed with anti-LRRK2 Ab (top panel). The expression levels of the transgenes are comparable among three lines. (b) Rearings in the cylinder test were counted for wild type non-transgenic littermates (WT, n=5) and WT-OX BAC mice (WT-OX, n=5). Contrary to *LRRK2*^{R1441G} mice, 10 month old WT-OX mice had slightly increased but not decreased motor activities compared to the non-transgenic littermate controls (p=0.024). Data are reported as mean ± s.e.m.

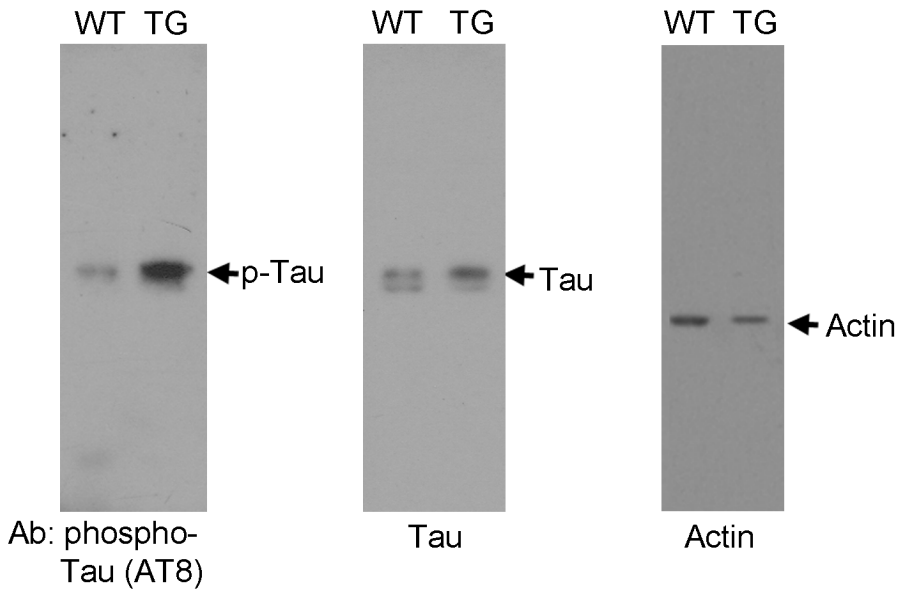

Supplementary Figure 7. Western analyses of tau and phospho-tau in brain lysates of *LRRK2*^{R1441G} BAC mice and non-transgenic littermates. Western blot was probed with anti-phospho-tau Ab (left panel), anti-tau Ab (middle panel) and anti-actin Ab (right panel). Hyperphosphorylation of tau is detected in the *LRRK2*^{R1441G} mouse brains

Supplementary Video legends

Supplementary Video. 1 Home cage behavior of 10 month old wild type non-transgenic littermates that moved normally, and *LRRK2*^{R1441G} BAC transgenic mice that became immobile (akinesia-like). The movie is real time. (Size: 1.5 Mb)

Supplementary Video. 2 Open field test of 10 month old wild type non-transgenic littermates that moved normally. The movie is real time. (Size: 2.3 Mb)

Supplementary Video. 3 Open field test of 10 month old *LRRK2*^{R1441G} BAC transgenic mice that became immobile. The movie is real time. (Size: 1.5 Mb)

Supplementary Video. 4 Cylinder test of 10 month old wild type non-transgenic littermates that moved and reared normally. The movie is real time. (Size: 1.4 Mb)

Supplementary Video. 5 Cylinder test of 10 month old *LRRK2*^{R1441G} BAC transgenic mice that became immobile. The movie is real time. (Size: 0.5 Mb)

Supplementary Video. 6 Rescue of the motor deficit in *LRRK2*^{R1441G} BAC transgenic mice by levodopa. Home cage behavior of 10 month old *LRRK2*^{R1441G} BAC transgenic mice about 1.5 hour post levodopa injection. There was a significant increase of motor activity. The movie is real time. (Size: 0.9 Mb)

Supplementary Video. 7 Rescue of the motor deficit in *LRRK2*^{R1441G} BAC transgenic mice by levodopa. Open field test of 10 month old *LRRK2*^{R1441G} BAC transgenic mice about 40 min post levodopa injection. There was a significant increase of motor activity. The movie is real time. (Size: 2.4 Mb)

Supplementary Video. 8 Rescue of the motor deficit in *LRRK2*^{R1441G} BAC transgenic mice by levodopa. Cylinder test of 10 month old *LRRK2*^{R1441G} BAC transgenic mice about 1 hour post levodopa injection. There was a significant increase of motor activity. The movie is real time. (Size: 6.7 Mb.)

Supplementary Method

Animal care:

All procedures are performed according to the guideline by Institutional Animal Care and Use Committee (IACUC) at Cornell University Medical College (CUMC).

BAC Screening, Modification and Confirmation

To obtain BACs that cover full length *hLRRK2* gene, 5'UTR and 3'UTR of *hLRRK2* cDNA were used as probes to screen a human BAC library (CHORI). A BAC clone was found to cover full-length *hLRRK2*. End sequencing revealed that this BAC has 29 kb upstream of start codon and 42 kb downstream of stop codon. Bioinformatics analysis predicted that there is no other gene within both the 29 Kb and 42 Kb regions. Fingerprinting analyses after digestion with restriction enzymes revealed no noticeable deletions in wild type *LRRK2* BAC. BAC modification was performed according to our standard protocols [1]. A second fingerprinting analysis demonstrated that there are no unwanted rearrangements or deletions in the modified $LRRK2^{R1441G}$ BACs. Finally, all the exons and exon-intron junctions were sequenced to confirm that there were no unwanted mutations other than the intended R1441G mutation.

hR1441G LRRK2 BAC Transgenic mice

$LRRK2^{R1441G}$ BACs were used for pronuclear injection in FVB background. Founders and progenies carrying $LRRK2^{R1441G}$ transgene were identified by PCR from tail DNA and direct sequencing. The full length $LRRK2^{R1441G}$ expression was confirmed by Western analysis. The transgenic mice were maintained by breeding to wild type

FVB mice. All the experiments performed with *LRRK2*^{R1441G} mice were controlled by wild type littermates kept in the same cage.

Western Analysis

Whole brain or different brain regions (cortex, midbrain, cerebellum, and striatum) were dissected from *LRRK2*^{R1441G} BAC transgenic mice, wild type *hLRRK2* overexpresser or wild type non-transgenic littermate controls, and homogenized in lysis buffer (0.32M Sucrose; 750 mM NaCl; 1 mM $NaHCO_3$; 20 mM HEPES, pH 7.4; 0.25 mM $CaCl_2$; 1 mM $MgCl_2$) containing 1X protease inhibitor cocktail (Roche) and 0.2 mM PMSF. The lysates were collected after centrifugation at 14,000 g for 15 min, and the protein concentration of each lysate was determined by DC protein assay (BIO-RAD). 50 μg of proteins were separated on a 4 -12% polyacrylamide gels and transferred onto PVDF membranes (Millipore). Western analyses were performed with anti-LRRK2 antibody (NB-300-267, Novus), anti-Tau (Santa Cruz), or anti-Phosph-Tau (AT8; Thermo scientific) followed by signal detection with enhanced chemiluminescence (Pierce). Actin and GAPDH were probed by antibodies against Actin (chemicon) or GAPDH (IMGENEX) respectively as internal controls for protein loading in Western blots.

Behavioral Testing

LRRK2^{R1441G}, wild type *hLRRK2* overexpresser mice and wild type non-transgenic littermates were kept in a 12:12 hour light/dark cycle in a temperature and humidity controlled room. All behavioral tests were conducted in the dark phase after two hours

of the light/dark switch. In home cage activity test, *LRRK2*^{R1441G} mice and wild type littermates were video taped in home cage for spontaneous ambulatory activity without any disturbance. In cylinder test, *LRRK2*^{R1441G} mice were individually transferred into a 12 cm diameter cylinder and video taped with a reflective mirror for 5 minutes. Vertical rearing and horizontal limb steps were counted. In open field test, mice were transferred into a 45 cm X 45 cm box for 10 minutes, video taped and analyzed by Ethovision 3.0 from Noldus. The locomotor activity was measured by total distance and the number of tiles that the mice traveled.

Pharmacological Rescue

LRRK2^{R1441G} mice and wild type littermates were injected with saline control or methyl levodopa hydrochloride (Sigma, St. Louis, USA) in 0.9% NaCl with benserazide 6.5 mg/kg (Sigma). Two dosages of methyl levodopa hydrochloride (2 mg/kg and 20 mg/kg) were tested. 0.3 ml of intraperitoneal injections was administered to each animal. Behavioral testings were performed 40 minutes after the injections. In addition, apomorphine (Sigma) was used at 10 mg/kg dosage by intraperitoneal injections. Behavioral testings were performed 5 minutes after the injections.

Microdialysis

Male *LRRK2*^{R1441G} transgenic mice or age-matched wild type non-transgenic littermates were anesthetized with a mixture of ketamine and xylazine and placed in a Kopf stereotaxic frame. A guide cannula (CMA/7, CMA Microdialysis, Sweden) was

implanted above the right striatum (AP +0.5, ML +1.7 from bregma, V -2.8mm from the dura) and secured with dental cement.

Microdialysis was performed 24 hours after surgery in free moving mice, using new CMA/7 probe (membrane: O.D. 0.24mm, 2mm length, 6000 Dalton cutoff). Ringer's solution (147 mM NaCl, 1.2 mM $CaCl_2$, 2.7 mM KCl, and 0.85 mM $MgCl_2$) was delivered at 1.5 µl/min (CMA/100 pump). Nomifensine maleate (100 µM) was dissolved in Ringer's solution. Dialysates were collected at 20 min intervals. 5 µl of perchloric acid (0.5 M) was added to sampling vials to prevent dopamine degradation. After 90-min equilibration period, three baseline samples were collected. Nomifensine was applied for 40 min, and the dialysates were collected for an additional 40 min with Ringer's solution. All samples were collected using a CMA/140 microfraction collector and then immediately frozen and kept at –80ºC until analysis.

Dopamine was analyzed using an ESA CoulArray detector (E_1 = −175 mV; E_2 = +325 mV; E_{guard} = 350 mV) (ESA, North Chelmsford, MA), with a 5014B microdialysis cell. Mobile phase (100 mM LiH_2PO_4, 10 mg/ml citric acid, 0.85 mM octanesulfonic acid, 5% acetonitrile, 5% methanol, PH 5.7) was delivered at 0.6 mL/min. C18 column (Tosoh Super ODS, 4.6×50 mm, 2 µ m) was kept at 42 °C. Data were analyzed by two-way ANOVA with repeated measures for Fig 2.

Immunohistochemistry for tyrosine hydroxylase in dopamine neurons in substantia nigra

Animals (9-10.5 month old) were perfused intracardially with 0.9% saline followed by 4% paraformaldehyde in 0.1M phosphate buffer. The brains were removed and blocked into forebrain and midbrain regions. The region containing the midbrain was post-fixed in the same fixative for one week. Each midbrain block was cryoprotected in 20% sucrose overnight and then rapidly frozen in isopentane on dry ice. A complete set of serial sections were cut through the substantia nigra at 30 μm and sections were placed individually in multiwell plates in serial order. Based on the fractionator method of sampling [2], sections were selected at a regular interval (every fourth) and processed free-floating with rabbit-anti-tyrosine hydroxylase (Calbiochem, La Jolla, CA) at 1:750. After treatment with biotinylated protein A, followed by avidin-biotinylated horseradish peroxidase complexes (ABC, Vector Labs, Burlingame, CA), and incubation with diaminobenzidine, sections were mounted onto slides and counterstained with thionin.

Immunohistochemistry for* tyrosine hydroxylase *in fibers in striatum and quantitative regional analysis

The forebrain region containing the striatum was post-fixed for 48 hours, rapidly frozen in isopentane on dry ice without cryprotection and cut at 30 μm from planes 3.94 to 4.90 mm (relative to interaural) [3]. Four representative sections from each plane were selected for tyrosine hydroxylase immunostaining as described for the substantia nigra. Sections were mounted and coverslipped. The optical density of striatal tyrosine hydroxylase staining was measured using an Imaging Research Analytical Imaging Station (St. Catherine, Ontario, Canada) under blinded conditions on coded slides.

Quantitative analysis of substantia nigra (A9) and ventral tegmental area (VTA) (A10) dopamine neuron numbers, neuron cross-sectional areas, SNpr* tyrosine hydroxylase-*positive fibers, and dystrophic* tyrosine hydroxylase-*positive neurites

Each complete set of tyrosine hydroxylase-immunostained serial stained sections was coded and analyzed by a stereological method for each animal under blind conditions. For each animal, one side of the brain was analyzed. The entire substantia nigra was defined as the region of interest. Using StereoInvestigator software (Micro Brightfield, Inc., Williston, VT), a fractionator probe was established for each section. The number of TH-positive neurons in each counting frame was determined by focusing down through the section using the optical dissector method under 100X oil-immersion objective. The criteria for counting an individual tyrosine hydroxylase-positive neuron was the presence of its nucleus either within the counting frame, or touching the right or the top lines (green), but not touching the left or the bottom lines (red). The total number of tyrosine hydroxylase-positive neurons and the total volume of the substantia nigra (in cubic microns) were determined by the StereoInvestigator software program. In a separate analysis, the same sections were used to determine the number of neurons in VTA. To ascertain tyrosine hydroxylase neuron cross-sectional area in the SNpc (A9), four representative rostral-caudal substantia nigra sections from each mouse were chosen. The first five tyrosine hydroxylase-positive neurons identified with a distinct nucleus and a complete cell body within randomly chosen sites distributed

across the medial to lateral dimension of the SNpc in each section were selected. For each neuron, the contour defined by tyrosine hydroxylase-positive cytoplasm and proximal tapering processes was outlined under a 100X oil-immersion objective, and the area (in square microns) was determined by the StereoInvestigator program. To obtain a measure of the number of tyrosine hydroxylase-positive fibers within the SNpr, a single substantia nigra anterior section containing the medial terminal nucleus of the accessory optic tract (MT) was chosen and analyzed under blind conditions on a coded slide. The entire SNpr was defined as the area of interest, excluding the ventral-most tier of SNpc tyrosine hydroxylase-positive neurons. The number of tyrosine hydroxylase-positive fibers in each counting frame was then determined by focusing down through the section at 100X under oil immersion. Any counting frame touching a tyrosine hydroxylase-positive cell body was omitted from the analysis, as they were operationally defined as within SNpc. The criterion for counting a fiber was any linear TH-positive fiber that intersected the upper horizontal line (green) of the counting frame.

In order to quantify dystrophic neurites in these brains, it was necessary to examine a region that contains tyrosine hydroxylase-positive axons, and yet does not also contain a dense plexus of tyrosine hydroxylase-positive neurites, because the latter would obscure dystrophic features at the single fiber level. Therefore, for this purpose, we selected the ventral pallidum. In order to reproducibly define the ventral pallidum as a region of interest, we selected only those sections derived from Paxinos and Franklin Planes 0.14 and 0.26 mm (Bregma) for the reason that the dorsal border of the ventral pallidum is discretely and distinctly defined by the transverse passage of the anterior

commissure in these planes. The lateral border of the region of interest was defined as the lateral-most extent of tyrosine hydroxylase staining of the olfactory tubercle, the medial border was defined as the mid-sagittal line, and ventral by the ventral surface of the brain. For this analysis, the number of objects of interest (dystrophic neurites) was too few to use the fractionator method of sampling. Therefore, in order to maximize the number of dystrophic neurites identified, we scanned at 600x the entire ventral pallidum bilaterally on 3 sections available form each mouse.

Anti-human paired helical filament-tau (AT-8) immunostaining in forebrain

Two representative coronal sections from each of the sampled interaural planes through the striatum were pre-treated with Mouse-on-Mouse Blocking Reagent (Vector Labs) and processed free-floating with a mouse monoclonal anti-human PHF-tau antibody (AT8)[4] (Pierce, Rockford, IL) at 1:100. Sections were incubated with biotinylated anti-mouse IgG reagent (Vector Labs), followed by ABC and diaminobenzidine chromogen reaction. In order to quantify AT8-positive neurites, a forebrain coronal section representing Paxinos and Franklin Plane 0.62 mm (Bregma), containing the striatum and the piriform cortex, was analyzed for each mouse. The striatum was scanned under blind conditions in its entirety at 600X, and adjacent piriform cortex was also scanned. The mean cross-sectional area of the striatum in the section was 5-6 mm^2 (see Figure 3b), and the adjacent piriform cortex was approximately 1.0 mm^2, for a total of 6-7 mm^2 scanned per brain.

References for Methods (on-line)

1. Gong, S., Yang, X. W., Li, C. & Heintz, N. Highly efficient modification of bacterial artificial chromosomes (BACs) using novel shuttle vectors containing the R6Kgamma origin of replication. Genome Research 12, 1992-8 (2002).
2. Coggeshall, R. E. & Lekan, H. A. Methods for determining numbers of cells and synapses: a case for more uniform standards of review. J Comp Neurol 364, 6-15 (1996).
3. Paxinos G, F. K. The Mouse Brain in Steereotaxic Coordinates (Academic Press, New York, 2001).
4. Biernat, J. et al. The switch of tau protein to an Alzheimer-like state includes the phosphorylation of two serine-proline motifs upstream of the microtubule binding region. Embo J 11, 1593-7 (1992).